Structural characterization of Ag_2GeS_3 glass by anomalous wide-angle x-ray scattering

P. Armand
LPMC, UMR 5617, Case 003, UMII, 34095 Montpellier Cedex 05, France

A. Ibanez and J.-M. Tonnerre
Lab. Cristallographie, CNRS, Boîte Postale 166, 38042 Grenoble Cedex 09, France

B. Bouchet-Fabre
LURE, Bât. 209D, 91405 Orsay, France

E. Philippot
LPMC, UMR 5617, Case 003, UMII, 34095 Montpellier Cedex 05, France

(Received 17 March 1997; revised manuscript received 20 June 1997)

Germanium and silver atomic surroundings of Ag_2GeS_3 glass have been studied by anomalous wide-angle x-ray scattering. The structural parameters deriving from the simulations of the differential distribution functions, characterizing selectively Ge and Ag environments, show that the medium-range order of the glass up to 5 Å is close to that of the crystallized reference α-Ag_8GeS_6. The absence of a first sharp diffraction peak on the structure factor around $Q=1$ Å^{-1}, can be explained by the lack of Ge-Ge correlations in the medium-range order. Finally, these results allow us to discuss the validity of several structural models proposed to explain the ionic conduction in glasses. [S0163-1829(97)08137-X]

I. INTRODUCTION

Germanium chalcogenide glasses of the Ag-Ge-S system are good solid electrolytes with a high Ag^+ ionic conduction at room temperature ($\sigma_{25\,°C}=1.35\times10^{-3}\,\Omega^{-1}\,cm^{-1}$).[1] Although this physical property has been well characterized for different glassy systems, the fundamental mechanisms of the ionic transport process are not yet fully understood from a microscopic point of view. This is partly due to a lack of structural information particularly in the medium-range order (MRO). For this reason, in order to establish correlations between the Ag^+ ionic conduction and the glassy structure, a structural determination of the Ag_2GeS_3 glass has been undertaken by anomalous wide-angle x-ray scattering (AWAXS) at room temperature.

At first, GeX_x ($X=$ S, Se) binary glasses have been characterized by x-ray-absorption spectroscopies,[2,3] extended x-ray-absorption fine structure (EXAFS), x-ray-absorption near-edge structure (XANES), AWAXS,[4] and small-angle x-ray scattering[5,6] (SAXS) experiments to follow afterwards the structural changes induced by the addition of silver sulfide as glassy network modifier in the $(1-y)GeS_2+yAg_2S$ ternary glasses.

The structural characterizations of $(1-y)GeS_2+yAg_2S$ glasses ($0.1\leqslant y\leqslant 0.5$) have been made following the same approach:

(i) Ge K-edge EXAFS studies at room temperature and 35 K have shown that the Ag_2S addition induces a simultaneous depolymerization of edge- and corner-sharing tetrahedra, which compose the g-GeS_2 structure, and an increase of short-range order (SRO) structural distortion.[2]

(ii) For Ag_2S-enriched glassy compositions ($y\geqslant 0.3$) the silver sites, characterized by Ag K-edge EXAFS analysis,[7] appear close to those of the α-Ag_8GeS_6 crystalline phase in agreement with other studies.[8,9] In this case, each silver atom is bonded to three sulfur atoms in very distorted sites. For low Ag_2S contents ($y<0.3$), the silver environment in the glasses is rather similar to that found in β-Ag_2S which has a lower average coordination number (2.5 sulfur atoms). Furthermore, S K-edge XANES spectra confirm that glasses with high silver proportions ($y\geqslant 0.3$) present sulfur environments closer to those encountered in the α-Ag_8GeS_6 crystal structure.[3]

(iii) In order to check the homogeneity of these ternary glasses, SAXS experiments have been performed.[5,10] For low Ag_2S contents ($y\leqslant 0.2$), the structure of these glasses is demixed, constituted by a glassy matrix based on the layered α-GeS_2 crystalline network and by Ag_2S aggregates of about 50 Å of diameter based on the structure of β-Ag_2S. When the proportion of silver sulfide increases, its ''dilution'' is improved due to the breaking of Ge-S-Ge linkages, as shown by Ge K-edge EXAFS, and thus, leads to smaller Ag_2S aggregates (Porod radius$\approx$20 Å). When the Ag_2S concentration increases, silver atoms are more uniformly distributed into the matrix, leading to a homogeneous glassy network ($y>0.3$).

To complete this structural characterization, x-ray-scattering experiments have been carried out. We report in this paper AWAXS results concerning the germanium and the silver surroundings of Ag_2GeS_3 glassy composition ($y=0.5$). This is followed by a discussion of the validity of various models suggested to explain the fundamental mechanisms involved in the ionic transport process on the basis of the glassy structure.

II. EXPERIMENTAL PROCEDURES

Since the procedure used in these measurements was very similar to that used in the germanium chalcogenide studies,[4]

only a short outline of the x-ray-scattering formalism, data acquisition, and data-analysis procedure will be given here.

A. Scattering formalism

In the following, the principle of the formalism is described for a binary alloy and it is straightforward to apply it for the ternary system. The normalized coherent x-ray-scattering intensity of noncrystalline materials whose components are A and B can be expressed as follows:

$$I(Q)-C_AC_Bf_A^2(Q)f_B^2(Q)=C_A^2f_A^2(Q)S_{AA}(Q)+C_B^2f_B^2(Q)S_{BB}(Q)+2C_AC_Bf_A(Q)f_B(Q)S_{AB}(Q), \quad (1)$$

where C_A and f_A are, respectively, the atomic ratio and the complex atomic scattering factor of the A species. $S_{AA}(Q)$, $S_{BB}(Q)$, and $S_{AB}(Q)$ are the partial structure factors of A-A, B-B, and A-B atomic pairs and Q is the scattering vector $(4\pi \sin\theta/\lambda)$.

If the incident photon energy is close to the energy of an absorption edge of a specific atom in the amorphous compound, there is a modification of the phase and amplitude of the electromagnetic wave so the atomic scattering factor is considered as a complex quantity:

$$f(Q,E)=f_0(Q)+f'(E)+if''(E). \quad (2)$$

Here, $f_0(Q)$ is the usual atomic scattering factor and f' and f'' are the anomalous scattering terms depending on the x-ray energy E.

The differential anomalous scattering (DAS) method, first used by Fuoss *et al.*,[11] takes advantage of the fact that f' and f'' change rapidly within ~ 100 eV around an absorption edge. The atomic structure around the central atoms A is expected to be obtained by taking the difference of two data sets collected just below (few eV) and far (several hundreds of eV) from the absorption edge of the A atom. So, the differential structure factor (DSF) obtained around the A edge, $\Delta_A S(Q)$, can be written as

$$\Delta_A S(Q)=\Delta[I(Q)-C_AC_Bf_A^2(Q)f_B^2(Q)]/2C_A\Delta f'_Af_{AB}(Q), \quad (3)$$

where f_{AB} is the average scattering factor of the system deduced from the two energies employed.

Then, by Fourier transformation of the DSF_A, we get the reduced differential distribution function ($RDDF_A$) and the differential distribution function (DDF_A) which determine selectively the atomic surroundings of atoms A:

$$\mathrm{RDDF}(r)=\mathbf{2}/\pi\int_0^\infty Q[\Delta_A S(Q)-\mathbf{1}]\mathbf{sin}(Qr)dQ, \quad (4)$$

$$\mathrm{DDF}=\mathbf{4}\pi r\rho_0+\mathbf{2}\pi r\int_0^\infty Q[\Delta_A S(Q)-\mathbf{1}]\mathbf{sin}(Qr)dQ. \quad (5)$$

TABLE I. Values of the anomalous scattering factors, f'' and f', used in this study for Ag_2GeS_3 glass at four different energies around the absorption K edge of germanium (11 103 eV) and silver (25 514 eV).

E (eV)	f''_{Ag}	f''_{Ge}	f''_S	f'_{Ag}	f'_{Ge}	f'_S
11 097	2.46	1.17	0.30	−0.34	−9.49	0.22
10 803	2.58	0.52	0.32	−0.31	−3.39	0.23
25 500	0.78	0.93	0.06	−6.40	0.19	0.03
24 434	0.60	0.99	0.06	−2.36	0.19	0.04

B. Experimental considerations

The glass synthesis was made in a silica ampoule sealed under high vacuum. The Ag_2GeS_3 phase was obtained from α-Ag_2S and g-GeS_2 compounds melted at 1000 °C during one week. The bulk glassy sample was obtained by the usual water-quenching method, and then annealed at 260 °C for 12 h to eliminate mechanical strains. The x-ray powder-diffraction technique was used to check the amorphous state. The specific mass, 5.086 g/cm^3, was obtained by pycnometry using benzene solvant. The atomic composition of the sample was determined by wave-dispersive x-ray fluorescence analysis which gave $Ag_{2.18}GeS_{3.06}$ molar composition.

The x-ray-scattering measurements were performed, at room temperature, on the W31B beamline of the DCI storage ring at LURE (Orsay). DCI was operated with a positron beam energy of 1.85 GeV and an average beam current of 250 mA. The AWAXS spectra were recorded on a powdered sample in the symmetric reflection mode (θ–2θ) on the two-circles goniometer at the Ge K-edge and asymmetric reflection mode ($\theta_{\mathrm{fixed}}=1.5°$) at the Ag K-edge. The monochromatization was carried out by a Si(220) double-crystal monochromator. The energy calibration was made using c-Ge for the scans around the Ge K-edge energy ($E=11\,103$ eV) and Ag foil for those around the Ag K-edge energy ($E=25\,514$ eV). The scattered intensities near and far from the absorption K-edge of germanium and silver, were measured by a Si:Li solid multidetector (10 detectors) cooled with liquid nitrogen.[12]

The values of the anomalous scattering factors f' and f'' (Table I) were extracted from Sasaki's tables[13] for the energies far from the Ge and Ag K-edges. Near the K-edge energies, f'' values were obtained from the x-ray-absorption spectra of the g-Ag_2GeS_3 phase. Then, the f' contributions were calculated using the Kramers-Krönig relationship.[14,15]

C. Data analysis

The same procedure as described in Ref. 4 has been followed for the data treatment. The scattered intensities were corrected from Compton scattering, geometrical factors, reabsorption phenomena, and, for data collected near the absorption edges ($E=11\,097$ and 25 500 eV), from the K_β fluorescence contribution. Then, from the absolute scattering intensities, we have determined the total structure factors (TSF's). The differential structure factors (DSF's) are obtained from the difference between the two measurements around an absorption edge. Finally, by Fourier transforma-

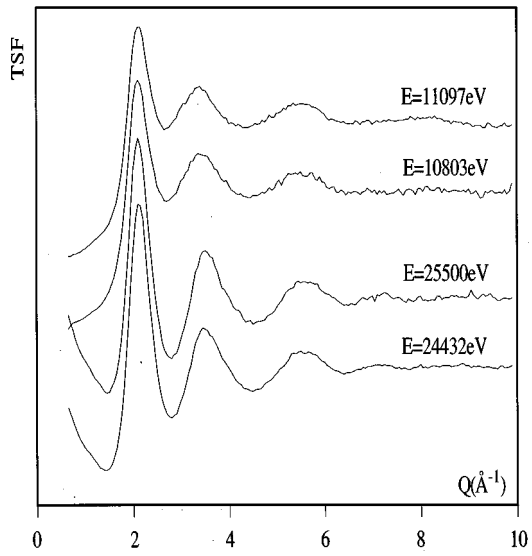

FIG. 1. Total structure factors collected at four different energies for g-Ag_2GeS_3. (The curves have been scaled for clarity.)

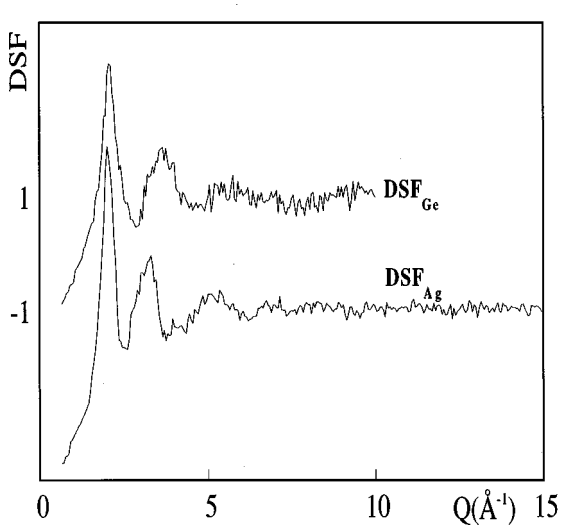

FIG. 2. Differential structure factors obtained around Ge (DSF_{Ge}) and Ag (DSF_{Ag}) K edges. (The curves have been scaled for clarity.)

tion of the DSF's, we have obtained the radial differential distribution functions (DDF's) characterizing selectively the Ge and Ag surroundings.

The real-space data can be analyzed by fitting Gaussian functions to the DDF, yielding the aera of each peak, its half-height width (σ), and also its position corresponding to the average interatomic distance R_{ij}. The coordination number $N_{i(j)}$ of j atoms about an average i atom can be derived from the aera. These simulations have to take into account the Q-dependant weight factors, $W_{ij}(Q)=c_ic_jf_if_j^*/\langle f\rangle^2$, of each partial structure factors, PSF_{ij}.

Furthermore, the number of variables in the fit should not exceed the number of relevant independent points in the experimental data given by, $N_{\text{ind}}=\Delta Q\Delta R/\pi$ where ΔQ and ΔR are the data ranges in the Q space (DSF's, Fig. 2) and in the R space [DDF's, Figs. 3(a) and 3(b)]. Around the germanium edge, $\Delta Q=9.5$ Å^{-1} and $\Delta R=7$ Å allow to refine 21 variables at the same time. For the silver edge, $N_{\text{ind}}=27$, since $\Delta Q=14.5$ Å^{-1} and $\Delta R=6$ Å. All the atomic subshells were fitted simultaneously in the 0–6, 7 Å range. Indeed, the structural parameters (N, R, and σ) of each coordination sphere are directly connected to their neighbors. Nevertheless, this difficulty is reduced by the fact that the weight factors, W_{ij}, of the atomic pairs are significantly different between themselves for the Ag_2GeS_3 glass. On the other hand, the extended data range involved in the real space ($\Delta R=6{,}7$ Å) for these fits reduces the problem of the cutting effects generally associated with the Fourier filtering.

The statistical errors of each structural parameter were estimated by different treatments carried out on independent spectra of the sample and by several simulation trials.

III. RESULTS

For each of the four experimental energies given in Sec. II and Table I, we have obtained the total structure factor (TSF) presented in Fig. 1 for g-Ag_2GeS_3. These curves are quite similar to each other and they do not exhibit a first sharp diffraction peak (FSDP) at about $Q=1$ Å^{-1} as that encountered on the TSF's of the glassy network former GeS_2.[16]

The differential structure factors (DSF's) were obtained around the germanium K-edge, DSF_{Ge} (difference between the TSF's obtained at $E=11\,097$ and 10 803 eV) and around the silver K-edge, DSF_{Ag} (difference between the TSF's obtained at $E=25\,500$ and 24 434 eV). DSF_{Ge} and DSF_{Ag} are plotted in Fig. 2.

The differential distribution functions (DDF's) around the germanium edge DDF_{Ge} and the silver edge DDF_{Ag} obtained by Fourier transform of the corresponding DSF, are shown in Fig. 3. These DDF's give selectively the average atomic surroundings of germanium (DSF_{Ge}) and silver (DSF_{Ag}) in g-Ag_2GeS_3.

Figures 4(a)–4(c) compare the germanium and the silver environments in g-Ag_2GeS_3, given by the DDF_{Ge} and the DDF_{Ag} curves, respectively, with those existing in α-GeS_2 and α-Ag_8GeS_6, which are represented by histograms. The aim of these comparisons is to allow an assignation of the kind of interatomic distances which could be involved in the DDF's. We note an important similarity between the Ge and Ag surroundings of g-Ag_2GeS_3 and α-Ag_8GeS_6, in good agreement with previous x-ray-absorption spectroscopy experiments carried out at the Ge, Ag, and S K-edges.[2,3,7] On the other hand, the Ge surroundings in g-Ag_2GeS_3 characterized by the DDF_{Ge} appear different from that of α-GeS_2, especially between 3 and 5 Å, Fig. 4(a).

Before discussing the germanium and silver environments in g-Ag_2GeS_3, we briefly review the crystalline structure of α-Ag_8GeS_6 and α-GeS_2 used as structural references. α-Ag_8GeS_6 (Ref. 17) is made up of isolated GeS_4 tetrahedra connected to sulfur and silver atoms to make a three-dimensional framework (Fig. 5). Among the eight independant Ag atoms, three types of silver coordination by sulfur atoms are observed: three Ag atoms are in a highly distorted tetrahedral environment, four are threefold coordinated while the last one is almost linearly linked to two S atoms. The Ge and Ag surroundings in this structure (coordination number and average distances) are, respectively, displayed in Tables II and III.

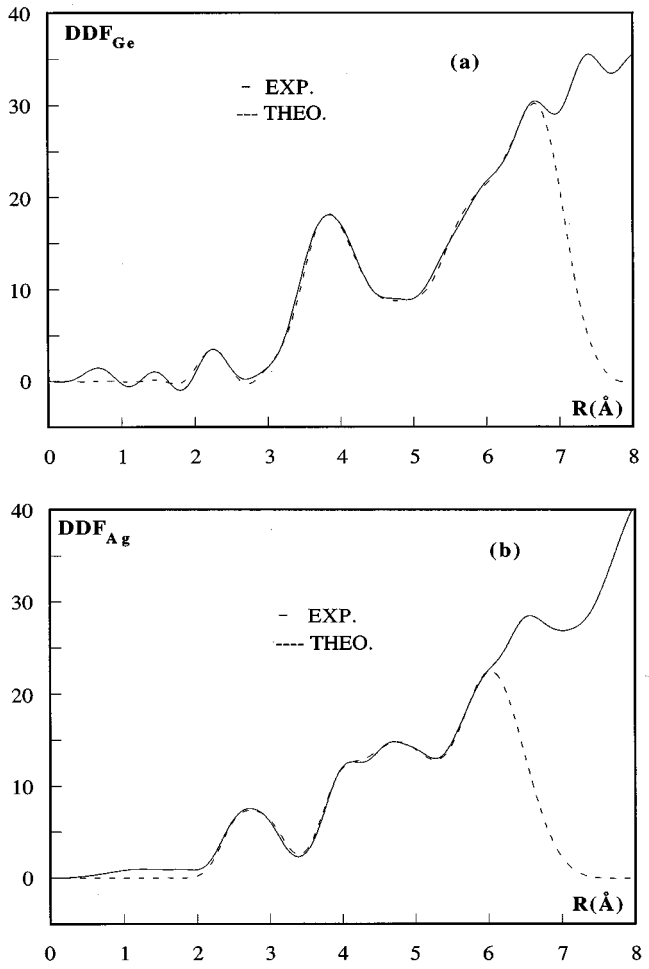

FIG. 3. Experimental and theoretical differential distribution functions characterizing (a) the Ge surroundings (DDF_{Ge}) and (b) the Ag ones (DDF_{Ag}).

α-GeS_2 has a layered structure[18] built up from $[GeS_3]_n$ chains of GeS_4 corner-sharing tetrahedra. These chains are connected through links of two edge-sharing tetrahedra, Fig. 6. The Ge environment in this reference (coordination number and average distances) is given in Table II.

A. Germanium environment

The DDF_{Ge}, related to the germanium atoms environment (correlations Ge-Ge, Ge-S, and Ge-Ag), has two principal peaks centered, respectively, at the distances of 2.3 and 3.9 Å, and a ''plateau'' between 4.4 and 5.0 Å, as shown in Fig. 3(a).

Due to the first comparison between the Ge surroundings in the glass and in α-GeS_2 and α-Ag_8GeS_6 references [Figs. 4(a) and 4(b)], we essentially based the simulations of the DDF_{Ge} curve on the average values of the Ge environment in α-Ag_8GeS_6 (Table II), but keeping in mind the chemical concentration difference between the glassy sample and the reference. The structural results obtained from the simulation are displayed in Table IV.

In the first coordination sphere, we find the typical tetrahedral surroundings of germanium with four Ge-S bonds ($N=3.8$) at 2.23 Å. To simplify the simulation of the second

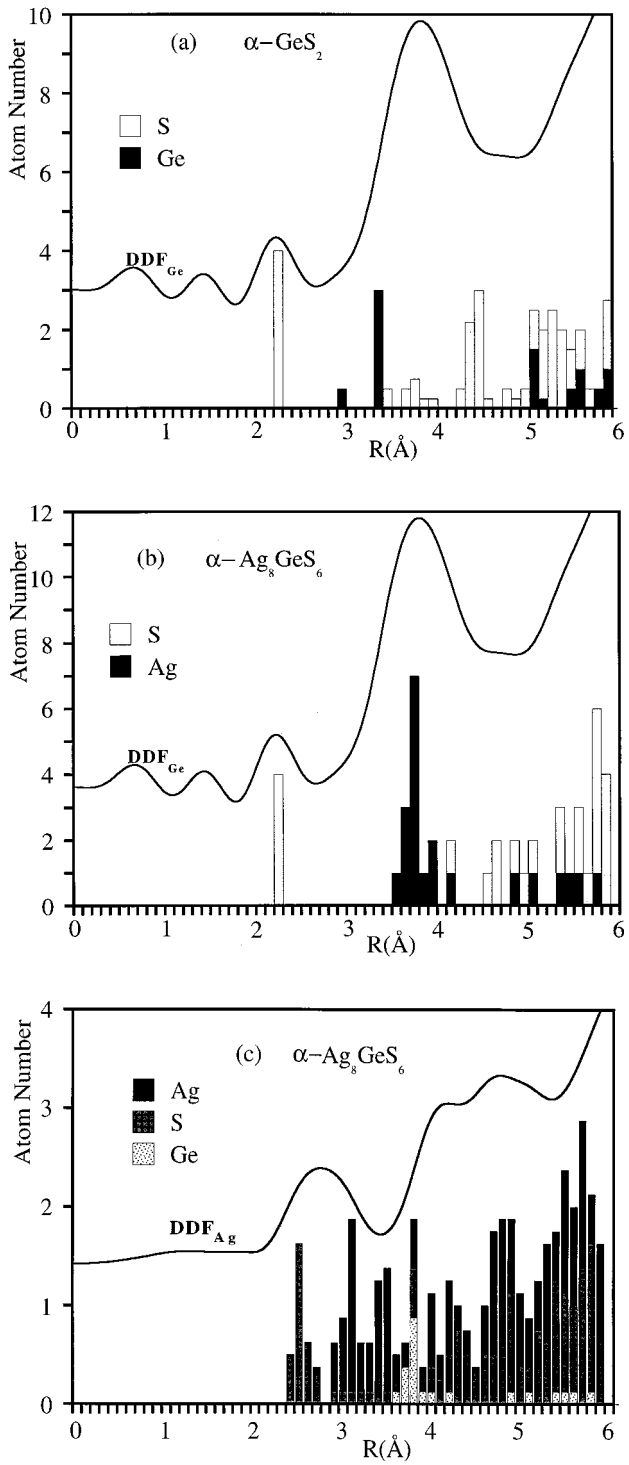

FIG. 4. Comparison of the germanium environment in g-Ag_2GeS_3, given by the DDF_{Ge} curve, with that existing in (a) α-GeS_2 and (b) α-Ag_8GeS_6, represented as histograms. In (c) the silver environment of the glass, DDF_{Ag}, is compared with that of α-Ag_8GeS_6.

peak of the DDF_{Ge} at 3.9 Å, we gathered in a unique atomic subshell centered at 3.85 Å with a large σ, all the Ge-Ag correlations ($N_{Ag}=10$) which are present in α-Ag_8GeS_6 between 3.7 and 4.2 Å (Table II). Moreover, to modelize the small contribution at $\sim$3 Å, we have involved the Ge...Ge interactions coming from edge (2.9 Å) and corner-sharing

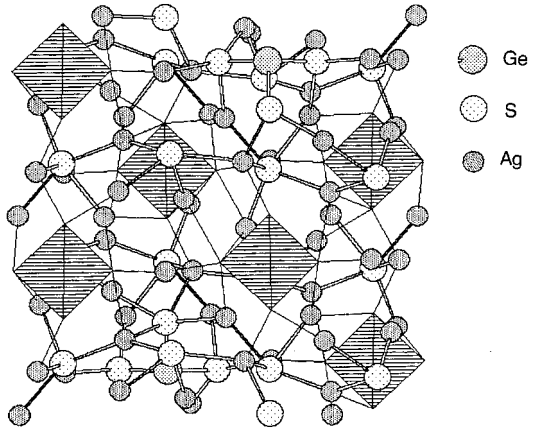

FIG. 5. Projection in the (a,b) plane of the α-Ag_8GeS_6 structure.

(3.4 Å) GeS_4 tetrahedra as existing in the reference α-GeS_2, Table II and Fig. 4(a). Indeed, due to the chemical composition difference between the studied glass Ag_2GeS_3 and the reference α-Ag_8GeS_6, Ge-Ge correlations have to be present. The coordination number obtained for the edge-shared tetrahedra ($N_{Ge}=0.2$ at $R=2.95$ Å) has not been considered in Table IV since it is on the order of the estimated error. On the other hand, concerning the corner-shared tetrahedra, we found non-negligible Ge-Ge correlations ($N_{Ge}=1.2$) at 3.55 Å (Table IV) referred to α-GeS_2 ($N_{Ge}=3$, $R=3.4$ Å, Table II).

In order to adjust the high R side of this second peak, 3.1 sulfur atoms located at a distance of 4.31 Å from germanium atoms were taken into account. The obtained coordination number ($N_S=3.1$) is justified by the fact that the chemical composition of the glass is richer in sulfur than the α-Ag_8GeS_6 phase.

The ''plateau'' ranging from 4.4 to about 5.0 Å, has been simulated using the interatomic distances of α-Ag_8GeS_6 (Table II). Two atomic subshells are constituted by sulfur atoms, one centered near 4.72 Å and the other near 5.04 Å, while a third one corresponds to silver atoms located around 5.0 Å, Table IV.

B. Silver environment

As shown in Fig. 3(b), the DDF_{Ag}, which contains Ag-Ge, Ag-S, and Ag-Ag correlations, presents three main peaks centered, respectively, at the distances of 2.8, 4.2, and 4.8 Å. As for DDF_{Ge} curve, we have mainly based the DDF_{Ag} analysis (until 5 Å) on the α-Ag_8GeS_6 (Table III) structure, taking also into account the DDF_{Ge} adjustment since the following relation should always be verified for heteropolar atomic pairs:

$$C_{Ge}N_{Ge\text{-}Ag}=C_{Ag}N_{Ag\text{-}Ge}, \tag{6}$$

where C represents the atomic concentration and N is the average coordination number.

The structural parameters obtained from the adjustment of the DDF_{Ag} curve are shown in Table V. The first broad peak (2–3.5 Å) has been reconstructed by three atomic subshells. One at $R=2.5$ Å with 3.3 Ag-S bonds corresponds to the nearest neighbors of the silver atoms. The second subshell contains 2.4 silver atoms at 2.9 Å, while the third one is due to 1.1 sulfur atoms centered at 3.0 Å. These two last subshells involve coordination numbers which are different from those observed in the reference (Table III) according to the chemical composition of the glass. Moreover, the correlation distances in g-Ag_2GeS_3 appear shorter than in α-Ag_8GeS_6.

The second peak of the DDF_{Ag} around 4.2 Å, corresponds to both Ag-Ge ($N_{Ge}=4.2$; $R=3.9$ Å) and Ag-Ag ($N_{Ag}=2$; $R=4.1$ Å) correlations (Table V) as existing in α-Ag_8GeS_6 (Table III). Furthermore, the Ag-Ge interactions correspond to the Ge-Ag ones [$N_{Ag}=10$; $R=3.85$ Å, (Table IV)] introduced in the modeling of the DDF_{Ge} [Eq. (6)].

Finally, the third peak centered at 4.8 Å was adjusted by still relying on the α-Ag_8GeS_6 structure and by using three

TABLE III. Average atomic distribution encountered around silver atoms in the crystalline reference α-Ag_8GeS_6.

	Atom type	N	R (Å)
	S	3.1	2.55
(0–3.6 Å)	Ag	6.3	3.20
	S	1.4	3.30
(3.6–4.4 Å)	Ge	1.8	3.90
	Ag	3.3	4.15
(4.4–5.3 Å)	S	5.0	4.45
	Ag	5.5	4.90
	S	6.0	5.05

TABLE II. Average structural parameters, coordination number N and distances R of Ge environment in the crystalline references α-Ag_8GeS_6 and α-GeS_2.

	α-Ag_8GeS_6			α-GeS_2		
	Atom type	N	R (Å)	Atom type	N	R (Å)
(0–2.9 Å)	S	4	2.23	S	4	2.22
(2.9–4.4 Å)	Ag	4	3.74	Ge	0.5	2.92
	Ag	7	3.85	Ge	3	3.40
	Ag	3	4.00	S	1	3.66
	Ag	1	4.26	S	1.25	3.90
	S	1	4.29	S	0.75	4.38
(4.4–5.0 Å)	S	3	4.71	S	4.5	4.5
	Ag	2	5.03	S	1.5	4.91
	S	3	5.07			

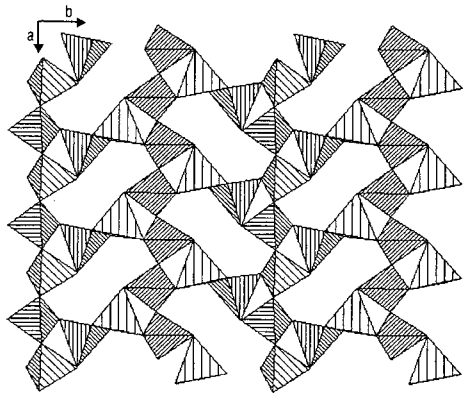

FIG. 6. Projection in the (a,b) plane of the α-GeS_2 structure.

atomic shells corresponding to Ag-S ($N=9$; $R=4.5$ Å), Ag-Ag ($N=1.7$; $R=4.8$ Å), and Ag-S correlations ($N=9$; $R=5$ Å), Table V.

IV. DISCUSSION

The AWAXS results obtained for g-Ag_2GeS_3 show that the germanium atoms are in tetrahedral sites surrounded by four sulfur atoms located at 2.23 Å and that the silver atoms are, on average, linked to 3.3 sulfur atoms at 2.5 Å. These results are in good agreement with previous studies made at both the Ge and Ag K edges[2,7] and show a high SRO similarity between the glass and α-Ag_8GeS_6. In addition, these structural results are consistent with those deriving from a neutron-diffraction study using an isotopic substitution on the same glass composition.[19]

Concerning the second coordination sphere of germanium, we found, in agreement with the chemical composition of the glass (Ag_2GeS_3), some Ge-Ge interactions corresponding to corner-sharing GeS_4 tetrahedra as present in the GeS_2 crystal (Fig. 6) and glassy structure.[2] However, the low coordination number found indicates that the Ag_2S addition induces an important depolymerization of the glassy matrix GeS_2 by breaking the corner- and edge-sharing tetrahedra, as already demonstrated by EXAFS Ge K-edge experiments.[2] Moreover, the presence of silver atoms in the second coordination shell of Ge (Table IV) indicates that the Ag atoms added to the glass former GeS_2 via the modifier Ag_2S are homogeneously incorporated at the atomic level into the glassy matrix.

The simulations made to reconstruct the atomic radial distribution function around both Ge and Ag edges confirm that the average structure of g-Ag_2GeS_3, in the range 2–5 Å is essentially based on that of the crystallized α-Ag_8GeS_6.

TABLE IV. Structural parameters obtained from the simulation of the DDF_{Ge} of the Ag_2GeS_3 glass.

DDF_{Ge}	Atom type	N	R (Å)	σ (Å)
First peak	S	3.8(3)	2.23(1)	0.16(1)
Second peak	Ge	1.2(4)	3.55(2)	0.25(2)
	Ag	10(2)	3.85(2)	0.38(2)
	S	3.1(8)	4.31(3)	0.30(2)
Plateau	S	2.0(5)	4.72(3)	0.30(3)
	Ag	1.4(4)	5.00(4)	0.32(3)
	S	2.3(5)	5.04(4)	0.33(4)

TABLE V. Structural parameters obtained from the simulation of the DDF_{Ag} of the Ag_2GeS_3 glass.

DDF_{Ag}	Atom type	N	R (Å)	σ (Å)
First peak	S	3.3(4)	2.5(3)	0.23(2)
	Ag	2.4(3)	2.9(3)	0.25(2)
	S	1.1(3)	3.0(3)	0.27(3)
Second peak	Ge	4.2(5)	3.9(3)	0.25(3)
	Ag	2.0(4)	4.1(3)	0.30(3)
Third peak	S	9(2)	4.5(3)	0.33(4)
	Ag	1.7(5)	4.8(4)	0.35(4)
	S	9(2)	5.0(4)	0.35(4)

A. First sharp diffraction peak

The first sharp diffraction peak (FSDP) is distinguished from other features in the structure factor in that the product of its wave vector Q_1 and the nearest-neighbor distance is almost universally found to lie in the range 2.2–2.8.[20] The structure factors for numerous amorphous phases and particularly for those of covalent systems such as Ge-Se,[4] Ge-S, As-P, P-Se (Ref. 20) present a FSDP situated around $Q \sim 1$ Å^{-1}. The origin of this first peak, which is the sign of a medium range order (MRO), has been the subject of widespread study and controversy.[21–25]

In previous studies on $GeSe_x$ ($x \geqslant 2$) glassy compositions,[4,26–29] the FSDP is displayed in the TSF curves but its intensity diminishes when the glass becomes rich in Se ($x>2$) and disappears completely beyond $x=5-6$. Further, for the differential structure factors, the FSDP presented in the DSF_{Ge} curve follows the same evolution. The structure of the glass former $GeSe_2$ is built up from edge- and corner-sharing $GeSe_4$ tetrahedra, while we observe a depolymerization of the $[GeSe_3]_n$ chains when the Se content increases ($x>2$) leading to isolated $GeSe_4$ tetrahedra for high Se concentrations ($x \geqslant 5$).[4] These structural results coupling with the FSDP behavior for these chalcogenide glasses suggest that the FSDP is mainly generated by Ge-Ge correlations in the MRO.[4]

In the same manner, for the glass former GeS_2, constituted of GeS_4 tetrahedra sharing edges and corners,[2] an intense first sharp diffraction peak is present at $Q=1.04$ Å on its structure factor[21] due to the presence of repetitive Ge-Ge correlations in the MRO. When Ag_2S is added to g-GeS_2 in the proportion 1:1, the FSDP vanishes (Fig. 1). The introduction of the glass modifier Ag_2S results in a significant degree of depolymerization of double and single bridged linkages (Ge-S-Ge). These linkages cannot be observed by EXAFS experiments even at 35 K[2]. In this case, the probability of having repetitive Ge-Ge correlations in the MRO is weak which explains the absence of a FSDP for the glass composition Ag_2GeS_3. In short, when the composition of the chalcogenide glass derives from the stoichiometric GeX_2 composition ($X=$ S, Se) by the addition of chal-

cogen or a modifier, the Ge-Ge order disappears due to an important depolymerization of edge- and corner-sharing GeX_4 tetrahedra.

B. Structural models

For complex glasses as ternary ones, no well defined structural models are available due to the lack of structural information. However, to explain the ionic transport process in glasses, three main models have been proposed.[30,32,34]

The modified random network model (MRN) developed by Greaves[30] is an extrapolation of the continuous random network model[31] for network oxide glasses. In the MRN model extension, the glass is constituted of zones built from the network former, separated from each other by more disturbed zones, the conduction channels, where the modifier cations (charge carriers) are present at high concentration.

For the cluster bypass model proposed by Ingram,[32] which is a modification of the broken chemical order model[33] for binary glasses, the glass structure is constituted by an unhomogeneous distribution of crystalline aggregates separated by modifier-enriched connective tissue giving the conduction paths.

In short, these two first models predict the existence of phase-separated glasses with a very low concentration of silver cations in the close environment of germanium atoms, in complete contradiction with our structural conclusions on Ag_2GeS_3 glass. Indeed, from SAXS (Refs. 5 and 10) and AWAXS experiments, the ionic transport process in this glass cannot be explained through silver-enriched pathways since the Ag^+ cations are homogeneously distributed in the glassy matrix with a high concentration of the latter close to each germanium atom ($N_{\text{Ge-Ag}}=10$ at 3.85 Å).

Our structural studies seem to support the third hypothesis developed by Elliott, the diffusion controlled relaxation model,[34] which suggests that ionic conductivity is induced by correlated jumps of the cation. This ionic transport process is probably promoted by a wide variety of sites for the Ag^+ charge carriers in the glassy structure.

V. CONCLUSIONS

The differential anomalous scattering method allowed us to characterize selectively the average atomic distribution of both germanium and silver atoms in the Ag_2GeS_3 glass. The structural parameters clearly demonstrate that their surroundings, in the 0–5 Å range, are essentially based on those found in the crystallized reference α-Ag_8GeS_6, in perfect agreement with the Ge, Ag, and S *K*-edges EXAFS results concerning the local range order.[3,7]

Moreover, the Ag^+ cations added to the former GeS_2 via the modifier Ag_2S are homogeneously incorporated, at the atomic level, into the glassy matrix since they are present as soon as the second coordination sphere of the Ge atoms (Table IV). We can suppose that the structure of the g-Ag_2GeS_3 would be constituted of GeS_4 tetrahedra mainly isolated from each others, surrounded by silver and sulfur atoms in a configuration rather similar to that encountered in α-Ag_8GeS_6.

Based on these structural considerations, the probability to find the same repetitive Ge-Ge correlations in the MRO is very weak. This will explain the disappearance of the FSDP in the structure factors of Ag_2GeS_3 glass. Furthermore, the ionic transport process in this glass cannot be explained by the MRN and cluster bypass models since they predict the existence of phase-separated glasses in complete disagreement with our structural conclusions,[3,5,7,10] which rather support the diffusion controlled relaxation model.[34]

[1] E. Robinel, B. Carette, and M. Ribes, J. Non-Cryst. Solids **51**, 49 (1983).

[2] P. Armand, A. Ibanez, H. Dexpert, and E. Philippot, J. Non-Cryst. Solids **139**, 137 (1992).

[3] P. Armand, A. Ibanez, and E. Philippot, J. Solid State Chem. **104**, 308 (1993).

[4] P. Armand, A. Ibanez, Q. Ma, D. Raoux, and E. Philippot, J. Non-Cryst. Solids **167**, 37 (1993).

[5] P. Armand, A. Ibanez, E. Philippot, D. Bittencourt, and C. Williams, J. Phys. IV **3**, C8-389 (1993).

[6] P. Armand, A. Ibanez, and E. Philippot, Nucl. Instrum. Methods Phys. Res. B **97**, 176 (1995).

[7] A. Ibanez, P. Armand, H. Dexpert, and E. Philippot, Solid State Ion. **59**, 157 (1993).

[8] L. C. Bourne, S. C. Rowland, and A. Bienenstock, J. Phys. C **4**, 951 (1981).

[9] R. J. Defus, S. Susman, K. J. Volin, D. Montague, and D. L. Price, J. Non-Cryst. Solids **141**, 162 (1992).

[10] P. Armand, A. Ibanez, J-M. Tonnerre, D. Raoux, B. Bouchet-Fabre, and E. Philippot, J. Non-Cryst. Solids **192&193**, 330 (1995).

[11] P. H. Fuoss, P. Eisenberg, W. K. Warburton, and A. Bienenstock, Phys. Rev. Lett. **46**, 1537 (1981).

[12] G. Nicoli, R. Andourart, C. Barbier, D. Dagneaux, M. de Santis, and D. Raoux, Soc. Ital. Fis. Conf. Proc. **25**, 353 (1990).

[13] (a) S. Sasaki, National Laboratory for High Energy Physics, KEK Report No. 83-28, 1983 (unpublished); (b) D. T. Cromer and D. Liberman, J. Chem. Phys. **53**, 1891 (1970).

[14] R. L. Krönig, J. Opt. Soc. Am. **12**, 547 (1926).

[15] H. A. Kramers, *Atti. Cong. Int. Fisici, Como-Pavia-Roma* (Zanichelli, Bologna, 1928), p. 545.

[16] L. Cervinka and J. Bergerova, J. Non-Cryst. Solids **150**, 132 (1992).

[17] G. Eulenberger, Monatsch. Chem. **108**, 901 (1977).

[18] Von G. Dittmar and H. Schäffer, Acta Crystallogr. Sect. B **31**, 2060 (1975).

[19] J. H. Lee, A. P. Owens, A. Pradel, A. C. Hannon, M. Ribes, and S. R. Elliott, J. Non-Cryst. Solids **192&193**, 57 (1995).

[20] S. C. Moss and D. L. Price, in *Physics of Disordered Materials*, edited by D. Adler, H. Fritzsche, and S. R. Ovshinsky (Plenum, New York, 1985), p. 77.

[21] S. R. Elliott, Phys. Rev. Lett. **67**, 711 (1991).

[22] P. S. Salmon, Proc. R. Soc. London, Ser. A **445**, 351 (1994).

[23] P. Vashishta, R. K. Kalia, and I. Ebbsjö, Phys. Rev. B **39**, 6034 (1989).

[24] P. Vashishta, R. K. Kalia, and I. Ebbsjö, Solid State Ion. **32/33**, 872 (1989).
[25] S. Susman, D. L. Price, K. J. Volin, R. J. Dejus, and D. G. Montague, J. Non-Cryst. Solids **106**, 26 (1988).
[26] P. H. Fuoss, P. Eisenberger, W. K. Warburton, and A. Bienenstock, Phys. Rev. Lett. **46**, 1537 (1981).
[27] P. Vashista, R. Kalia, G. Antonio, J. Rino, H. Iyetomi, and I. Ebbsjö, Solid State Ion. **40/41**, 175 (1990).
[28] J. C. Malaurent and J. Dixmier, J. Non-Cryst. Solids **35&36**, 1227 (1980).
[29] N. Ramesh Rao, K. S. Sangunni, E. S. R. Gopal, P. S. R. Krishna, R. Chakravarthy, and B. A. Dasannacharya, Physica B **213&214**, 561 (1995).
[30] G. N. Greaves, J. Non-Cryst. Solids **71**, 203 (1985).
[31] W. H. Zachariasen, J. Am. Chem. Soc. **54**, 3841 (1932).
[32] M. D. Ingram, Philos. Mag. B **60**, 729 (1989).
[33] J. C. Phillips, J. Non-Cryst. Solids **43**, 37 (1981).
[34] S. R. Elliott, Phys. Rev. B **41**, 47 (1991).